



## Photocatalytic activity of $X\text{InS}_2$ (X: Ag, Cu) nanoparticles for oxidative desulfurization of diesel fuel

Pham Xuan Nui<sup>1,\*</sup>, Ngo Thanh Hai<sup>1</sup>, Vu Van Toan<sup>1</sup>, Cong Tien Dung<sup>2</sup>, Le Thi Phuong Thao<sup>2</sup>

<sup>1</sup> Department of Chemical Engineering, Faculty of Petroleum and Energy, Hanoi University of Mining and Geology, 18 Pho Vien, Duc Thang, Bac Tu Liem district, Hanoi, Vietnam

<sup>2</sup> Department of Chemistry, Faculty of Basic Science, Hanoi University of Mining and Geology

\*Email: [phamxuannui@humg.edu.vn](mailto:phamxuannui@humg.edu.vn)

### ARTICLE INFO

Received: 05/08/2024

Accepted: 13/09/2024

Published: 30/09/2024

#### Keywords:

Ag(Cu)InS<sub>2</sub>; oxidative desulfurization; photocatalysts; dibenzothiophene; diesel fuel

### ABSTRACT

In this work, Ag(Cu)InS<sub>2</sub> semiconductor nanoparticles were synthesized via microwave and solvothermal methods. The effects of synthetical parameters on the structure and morphology of the nanoparticles were characterized by XRD, SEM, TEM, UV–Vis, and EDX. The experimental results reveal that the AgInS<sub>2</sub> compound can be crystallized in two different phases, which are tetragonal and orthorhombic. The nanoparticles size of AgInS<sub>2</sub> is about 15-16 nm and the direct band gap energy ( $E_g$ ) of 2.041. While CuInS<sub>2</sub> has the average particle size of around 25 nm and  $E_g$  value of 3.38 eV. The catalytic activity of both AgInS<sub>2</sub> and CuInS<sub>2</sub> materials were performed for photocatalytic oxidative desulfurization of sulfur compounds in the commercial diesel fuel under visible light. The maximum oxidation efficiency of 98.05% was achieved for AgInS<sub>2</sub> catalyst after 8 hours of reaction time.

## 1. Introduction

Sulfur-containing organic compounds in liquid hydrocarbon fuels are known as a cause of air pollution and acidic rain due to the release of sulfur oxides (SO<sub>x</sub>) during the process of fuel combustion. Nowadays, many countries promulgated the rules demanding to minimize the amount of sulfur in the fuel [1-5]. In modern industry, hydrodesulfurization (HDS) has been employed. However, this technology required the performance in high pressure and temperature conditions, and consumed significant amounts of hydrogen. Moreover, it is very difficult to remove dibenzothiophene (DBT) and their derivatives by that way because of the presence of the aromatic rings in the molecules that makes the increase in aromatic properties [6, 7]. Several other methods has been

widely investigated by scientists such as biodesulfurization (BDS) [8], adsorption desulfurization (ADS) [9], oxidative desulfurization (ODS) [10] in order to achieve deep desulfurization with the threshold limit for sulfur in diesel fuel is expected to be regulated to 5 ppm of weight (ppmw). Among these methods, the process of oxidative desulfurization (ODS) is one of the effective methods supplementing the HDS [10-12]. Under this process, the sulfide can be converted to SO<sub>4</sub><sup>2-</sup>, SO<sub>2</sub> or the sulfones, and then be absorbed by the alkaline solution, silica-gel or extracted by polar solvents [13].

Among the methods of oxidative desulfurization, photocatalytic oxidative desulfurization is the method having several advantages compared to the traditional methods, in which the operation is in mild conditions such as low temperature (<100°C), atmospheric

pressure (~1 atm), and absence of hydrogen gas [14-16]. TiO<sub>2</sub> was well-known as photocatalyst for oxidative desulfurization of sulfur-containing organic compounds such as thiophene, benzothiophene and the treatment efficiency of 86% was observed [17-19]. However, there are two issues raised when TiO<sub>2</sub> is used as a photocatalyst. Firstly, the super aggregation of catalysts existing at the form of very fine powders could occur. Secondly, TiO<sub>2</sub> catalyst has high band gap energies ( $E_g = 3.2\text{--}3.8$  eV). It means that it can only be excited by ultraviolet region ( $\lambda < 400$  nm) which accounts for only approximately 4% in the solar light, while the main part in the solar light is the visible region which obtains up to 35% of the energy [20, 21].

E.S. Aazam [22] studied nanocatalyst of Ag-TiO<sub>2</sub> supported on multi-walled carbon nanotubes (MWCNT) and used to treat the thiophene by photocatalytic oxidative reaction under visible light ( $\lambda > 400$  nm). The results indicated that both Ag and TiO<sub>2</sub> nanoparticles were well-dispersed over the multi-walled carbon nanotubes. The impregnated silver can eliminate the recombination of electron-hole pairs in the catalyst, and the presence of multi-walled carbon nanotubes TiO<sub>2</sub> composite could change the surface properties to achieve sensitivity to visible light. Chao Wang *et al.* [23] prepared the TiO<sub>2</sub>/g-C<sub>3</sub>N<sub>4</sub> photocatalyst with different weight ratios by two-step method. Photocatalytic activities of the samples were investigated by photocatalytic oxidative reaction of dibenzothiophene (DBT). The results showed that the removal of DBT could be achieved up to 98.9% in optimal condition after 2h of reaction time at room temperature. Thu Ha Thi Vu *et al.* [24] carried out synthesizing photocatalytic composite of multi-walled carbon nanotubes on TiO<sub>2</sub>. Using the obtained composite as a photocatalyst, more than 98% of sulfur compounds in commercial diesel were removed.

Recently, the presence of ternary chalcogenides of XY<sub>m</sub>Z<sub>n</sub> (X=Cu, Ag, Zn, Cd; Y= Ga, In; Z=S, Se,Te;  $m, n$ =integer) has great attention of the researchers due to their excellent electrical [25] and photochemical properties [26]. These materials have been applied in several fields such as photovoltaic solar cells [27], linear and non-linear optical instruments and photocatalytic processes [28, 29], .... One of the ternary chalcogenide photocatalyst, AgInS<sub>2</sub>, is an attractive material due to its high promising applications in photovoltaic, opto-electronic, and especially in photocatalytic field. E.S. Aazam *et al.* [30] prepared AgInS<sub>2</sub> nanoparticles by microwave assisted method and the obtained catalysts

were carried out for photocatalytic oxidation of cyanide under visible light. The results showed that oxidation efficiency of 100% was achieved with 1.5 wt% Pt/AgInS<sub>2</sub> photocatalyst.

In this work, we synthesized the XInS<sub>2</sub> (X: Ag, Cu) nanoparticles by hydrothermal method and evaluated their photocatalytic activity for oxidative desulfurization of dibenzothiophene (DBT) as a model fuel and commercial diesel fuel. Characteristics of the synthesized nanoparticles were analyzed by X-ray diffraction (XRD), scanning electron microscopy (SEM), and ultraviolet-visible spectroscopy (UV-Vis).

## 2. Experimental

All the chemicals used in this study were purchased from Aldrich and used without further purification. The procedure of XInS<sub>2</sub> synthesis was carried out according to our previous study [31, 32]. Briefly, the AgInS<sub>2</sub> nanoparticles were prepared as follows: 5 mmol sodium dodecyl sulfate (Aldrich; 99.5%) as surfactant dissolved in 50 mL of ethylene glycol at 80 °C for 15 min. An aqueous solution of 1 mmol AgNO<sub>3</sub> (Aldrich; 99.5%), 1 mmol InCl<sub>3</sub> (Aldrich; 99.5%), and 5 mmol thioacetamide (Aldrich; 99.5%) were added to the above solution and vigorously stirred for 30 min to become a homogeneous solution and adjusted the pH to value of 4 by using 1.0 M HCl to obtain solution A. This solution was performed by solvothermal methods. The above solution was introduced into a 250 mL Teflon-lined autoclave and followed by placing into an oven for 24 hours at temperature reaction of 180 °C. After cooling the Teflon-lined container to room temperature, the obtained solid material was washed several times by distilled water, and then by absolute ethanol. The sample was finally dried under a vacuum at 80 °C for 5h.

### *Synthesis of CuInS<sub>2</sub> nanoparticles*

CuInS<sub>2</sub> nanoparticles were synthesized by solvothermal method, in which the steps just followed the synthesis procedure of AgInS<sub>2</sub>. In this procedure, 5 mmol sodium dodecyl sulfate was dissolved in 50 mL of ethylene glycol (EG) in a flask and vigorously stirred at 80 °C in 15 min. An aqueous solution of 1 mmol CuCl (Aldrich; 99.5%), 1 mmol InCl<sub>3</sub>, and 5 mmol TAA was added to the above solution and vigorously stirred for 30 min to become a homogeneous solution. The final solution was introduced into a 250 mL Teflon-lined autoclave and heated at 180 °C for 24 h. The obtained precipitate was thoroughly washed by distilled water and absolute

ethanol. Finally, the sample was dried under the vacuum at 80 °C for 5 h. The mole ratio of the chemicals was 1CuCl:1InCl<sub>3</sub>:2TAA. The sample was assigned as CIS-180.

### Characterization

The crystalline phase structure of materials was determined by X-ray diffraction (XRD) using a Bruker D8 advance diffractometer with Cu-K $\alpha$  radiation ( $\lambda = 1.5406 \text{ \AA}$ ) operating at 40 mA and 40 kV, and the diffraction patterns were measured in the  $2\theta$  range of 20 - 70°. The surface morphology of catalysts was observed by scanning electron microscopy (SEM) using an S-4800 microscopy (Hitachi, Japan). The band gap of AIS, CIS photocatalysts was identified using Ultraviolet-Visible spectroscopy (UV-Vis) on spectrophotometer (V-670, JASCO, Japan) measured at room temperature in the air and in the wavelength range of 200–800 nm. From the value of wavelength absorption maximum ( $\lambda_{max}$ ) and using Planck's law, the band gap energy ( $E_g$ ) was determined from the following equation as  $E_g = hc/\lambda_{max}$ , where,  $h$  is Planck's constant;  $h = 6.625 \times 10^{-34} \text{ J.s}$ ;  $c = 3 \times 10^8 \text{ m.s}^{-1}$  is transmission speed of light in vacuum.

### Photocatalytic activity

#### Photocatalytic activity with DBT

To determine the products of photocatalytic reaction of commercial diesel sample, dibenzothiophene (DBT) was used as the model fuel. Model fuel with S-content of 600 ppm was prepared by dissolving calculated amount of DBT in *n*-octane. In a typical reaction, 0.2 gram of AIS-24 photocatalyst, 20 mL model oil, and 2 mL of H<sub>2</sub>O<sub>2</sub> as the oxidative agent were put into a 250 mL 3-neck flask at temperature 70 °C. The mixed solution was placed in the dark for 30 min to establish adsorption-desorption equilibrium. After that, the suspension solution was irradiated for 5 hours by a 160 W lamp of high-pressure mercury vapor as the light source. The reaction solutions were taken and separated by high-speed centrifuge. The products of reaction solution were analyzed by Gas Chromatograph–Mass Spectrometer (GC–MS) (Agilent 7890/5975C-GC/MSD; HP-5 MS column, 30 m  $\times$  0.25 mm  $\times$  0.25  $\mu$ m) with the temperature program: rising from 100 °C to 250 °C with the rate of 10 °C/min and keep the temperature at 250 °C for 10 min.

#### Photocatalytic activity with commercial diesel

Photocatalytic oxidation reaction of commercial diesel samples with total sulfur content of 615.62 ppm was performed with the same procedure conditions

conducted for DBT model fuel above. AIS-24 or CIS was used as the catalysts for desulfurization in different reaction times. After the photocatalytic reaction, the catalysts were separated by the centrifuge and the reaction products were absorbed by the column containing silica-gel and its content of sulfur was determined by X-ray fluorescence (XRF) (TS-100V, Mitsubishi, Japan) according to ASTM D-1266-13.

## 3. Results and discussion

### The structural characteristics of $X\text{InS}_2$ ( $X$ : Ag, Cu) photocatalysts

Figure 1 indicates X-ray diffraction patterns of the synthesized  $X\text{InS}_2$  nanoparticles. The XRD pattern shown in Figure 1(a) is related to the synthesized AIS sample, the characteristics peaks at  $2\theta$  values of 26.8°, 44.9° and 52.4° were identified as the tetragonal AIS crystal planes of (112), (204) and (312), respectively. The diffraction peaks at 24.9°, 25.4°, 26.6°, 44.5°, 48.2° and 53.1° were assigned to (120), (200), (002), (040), (123), and (400) planes of the orthorhombic AIS crystal phases, respectively (JCPDS 00-025-1330).

The XRD pattern of CIS nanoparticles, which were also prepared by the solvothermal method at 180 °C in 24 h, is shown in Figure 1b. Several prominent XRD peaks were identified as the CIS crystal planes of (112), (200), (220) and (215) of pure tetragonal CIS phase that are at  $2\theta$  values of 27.8°, 34.6, 46.5° and 54.8°, respectively (JCPDS card No. 38-0777). This XRD result is highly consistent with those published in articles for CIS [33, 34]. In addition, XRD peaks are broaden, confirming that CIS nanoparticles sizes are very small.

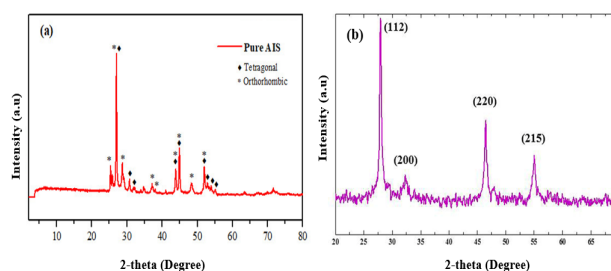


Fig. 1: X-ray diffraction patterns of (a) AIS and (b) CIS synthesized by solvothermal method

Figure 2(a,b) shows that the morphology of AIS nanoparticles, in low magnification, has the shape of a large number of mesh spheres combined together with the diamond-shape voids directed toward the center of the spheres, whose diameter varies from 2 to 4  $\mu$ m. There is no appearance of other morphologies

observed. This indicates the formation of the only 3D nanospheres. The intergrowth of nanoplates produced a large number of the spheres in nano range with ordered micropores. Besides, the morphology of the synthesized CIS nanoparticles were observed by SEM image (Figure 2(c,d)). As shown in Figure 2(c,d) nanoparticles of CIS aggregated to form uniform spheres. From the SEM results, it can be seen that the flower-shaped microspheres of  $XInS_2$  have a rough surface morphology leading to a layer structure, which provides a lot of surface area that increases visible light irradiation promoting photo-generated electron-hole ( $\bar{e}/h^+$ ) generation in these photocatalyst systems.

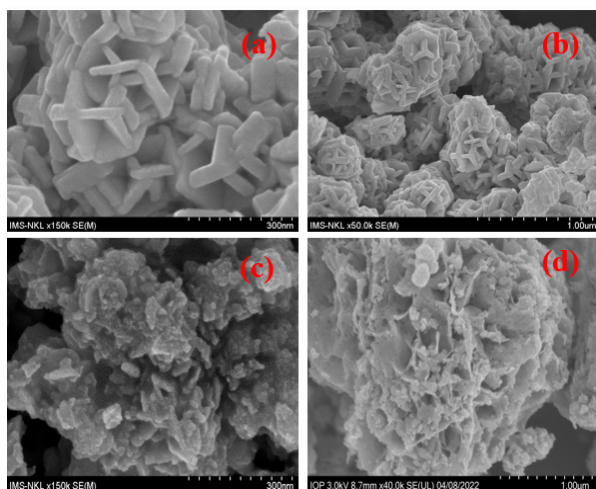


Fig. 2: SEM images of (a,b) AIS and (c,d) CIS nanoparticles

To determine the chemical composition of the synthesized AIS nanoparticles, energy dispersive spectroscopy (EDS) analysis was utilized. The results of EDS analysis indicate that the nanoparticles had an average  $X:In:S$  composition is near the target 0.25:0.25:0.5 ratio. Therefore, the formula of multi-component nanoparticles of  $XInS_2$  could be confirmed.

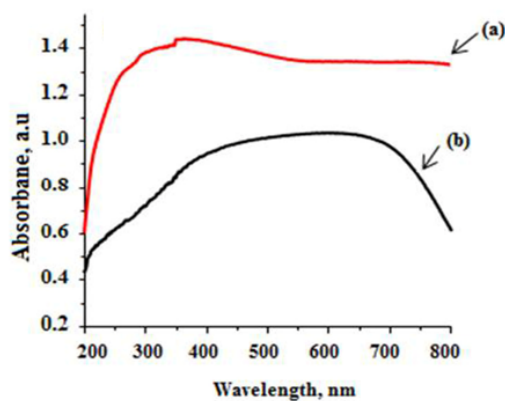


Fig. 3: UV-Vis absorption spectra of (a) AIS and (b) CIS nanoparticles

It is important to mention that synthesis methods have a significant effect on photocatalytic activity of materials. Figure 3 shows the absorption spectra of AIS and CIS samples prepared by varying the element of the precursors while keeping the other reaction conditions. Accordingly, the optical band-gap increases from 2.041 eV (AIS) to 3.380 eV (CIS), suggesting that the changing in the particle size of the precursors greatly influences on the size and size distribution of the resulting nanoparticles.

### Photocatalytic activity

#### Photocatalytic activity for oxidative desulfurization of dibenzothiophene (DBT)

To determine the products of photocatalytic reaction of commercial diesel sample, the photocatalytic reaction of DBT as the model fuel was performed over AIS-24 catalyst. DBT was oxidized to dibenzothiophene sulfone (DBT- $O_2$ ) that was confirmed from fragmentation peaks of mass spectrum at  $m/z$  216 and 187 in Figure 4. There was no peak at  $m/z$  200 symbolizing for dibenzothiophene 5-oxide. After sulfur compounds have been oxidized to sulfones which are easier to adsorb [24], they are undergone to adsorption by silica-gel for deep desulfurization.

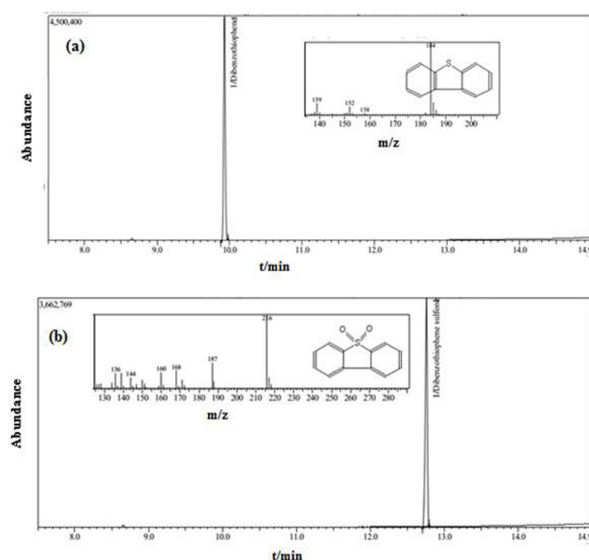


Fig. 4: The GC-MS of the oxidative product of DBT by AIS photocatalyst: (a) Dibenzothiophene, (b) Dibenzothiophene sulfone.

With the effect of  $XInS_2$  photocatalyst dosage on oxidative desulfurization of DBT under sunlight irradiation, according to our previous study [36], increasing the amount of photocatalyst leads to an increase in the photodegradation of DBT. This is due to the increased catalytic active sites could enhance the

generation and transfer of photogenerated charge carriers. However, if the photocatalyst dosage continually increased, the interaction among the outer layers of the catalyst reduced the photon formation of the inner layers, leading to a decrease in the separation of the photogenerated electron and hole pairs, thus reducing the photocatalytic efficiency [37].

#### Photocatalytic activity of desulfurization of commercial diesel

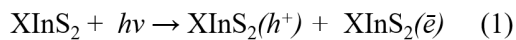
The relationship between the sulfur content in commercial diesel and reaction time using AIS photocatalyst is shown in Table 1(a). The results show that the efficiency of sulfur treatment process in DO fuel was observed after 1 h of reaction. The sulfur content in commercial diesel of 615.62 ppmw was decreased to 280.07 ppmw. When the reaction time was increased from 1 h to 3 h, the sulfur remaining content was about 60.00 ppmw. And up to 5 h, this content was decreased to 57.46 ppmw. The efficiency of the reaction increased from 25.44 to 84.71%, respectively. It could be seen that as the reaction time was up to 8 h, the sulfur remaining content was only 12.23 ppmw that corresponds to the efficiency of 98.01%.

Table 1: The total sulfur content obtained with different reaction times over AIS photocatalyst

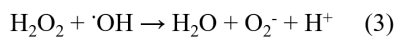
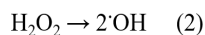
Reaction time (h)	The total S-content (ppmw)	Conversion efficiency (%)
0	615.62	-
1	280.07	25.44
3	60.00	84.03
5	57.46	84.71
8	12.23	98.01

Based on the conditions carried out for photocatalytic oxidation of commercial diesel over AIS catalyst, activity of the CIS catalyst was also performed. The results are shown in Table 1. Under the same reaction conditions, the efficiency of photocatalytic oxidation of AIS catalyst (98.01%) was higher than that of CIS catalyst (90.65%), indicating that the material of AIS nanoparticles with more narrow band-gap energy would enhance the adsorption ability in visible light, and possess the effective separation of photo-generated charge. Therefore, the AIS may be a suitable candidate as the catalyst for oxidative desulfurization of diesel fuel.

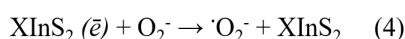
Thus, under visible light irradiation, charge carriers were created from photoexcitation of  $XInS_2$  can rapidly undergo redox reactions according to Eq. 1.



Besides,  $H_2O_2$  is a strong oxidizing agent that when exposed to visible light produces hydroxyl radical ( $\cdot OH$ ) (Eq. 2). Then, the reaction between  $H_2O_2$  and hydroxyl radicals from anion oxygen (Eq. 3) [35]:



These anion oxygens  $O_2^-$  absorbed on the  $XInS_2$  surface to produce strong oxidizing and active  $\cdot O_2^-$  as following Eq. 4.



Model of photocatalytic oxidative desulfurization of DBT using photocatalysts  $XInS_2$  under visible light irradiation is shown in Fig.5.

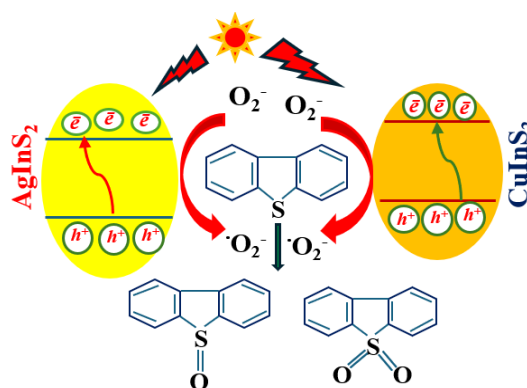


Fig. 5: Model of photocatalytic oxidative desulfurization of DBT using photocatalysts  $XInS_2$  under visible light irradiation

## 4. Conclusion

Nano sulfide materials with multi-metal components ( $XInS_2$  (X: Ag, Cu)) were successfully synthesized by solvothermal methods. The formation of  $XIS_2$  photocatalysts in two different structural phases with average particle size of 15-16 nm, the band gap energy ( $E_g$ ) in the range of 2.041 was observed. CIS photocatalyst with the average particle size of 25 nm and the  $E_g=3.38$  eV was also prepared. Dibenzothiophene sulfone is the product of the photocatalytic desulfurization of DBT. AIS is an appropriate for removal of sulfur from commercial diesel.

## Acknowledgement

The authors would like to thanks the financial support of National Foundation for Science and Technology Development (Nafosted), Code 105.99-2023.01.

<https://doi.org/10.62239/jca.2024.050>

## References

- J. Zhang, K. He, Y. Ge, X. Shi, *Fuel* 88 (2009) 504. <http://dx.doi.org/10.1016/j.fuel.2008.09.001>
- B. Zielinska, J. Sagebiel, J.D. McDonald, K. Whitney, D.R. Lawson, *J. Air Waste Manage. Assoc.* 54 (2004) 1138. <http://doi.org/10.1080/10473289.2004.10470973>
- M.M. Maricq, R.E. Chase, N. Xu, D.H. Podsiadlik, *Environ. Sci. Technol.* 36 (2002) 276. <http://doi.org/10.1021/es010961t>
- S.D. Shah, D.R. Cocker, J.W. Miller, J.M. Norbeck, *Environ. Sci. Technol.* 38 (2004) 2544. <http://doi.org/10.1021/es0350583>
- P. Saiyasitpanich, M. Lu, T.C. Keener, F. Liang, S.-J. Khang, *J. Air Waste Manage. Assoc.* 55 (2005) 993. <http://doi.org/10.1080/10473289.2005.10464685>
- Z. Deng, T. Wang, Z. Wang, *Chem. Eng. Sci.* 65 (2010) 480. <http://dx.doi.org/10.1016/j.ces.2009.05.046>
- M. Houalla, D.H. Broderick, A.V. Sapre, N.K. Nag, V.H.J. de Beer, B.C. Gates, H. Kwart, *J. Catal.* 61 (1980) 523. [http://dx.doi.org/10.1016/0021-9517\(80\)90400-5](http://dx.doi.org/10.1016/0021-9517(80)90400-5)
- S. Guchhait, D. Biswas, P. Bhattacharya, R. Chowdhury, *Chem. Eng. J.* 112 (2005) 145. <http://dx.doi.org/10.1016/j.cej.2005.05.006>
- Y. Shen, P. Li, X. Xu, H. Liu, *RSC Adv.* 2 (2012) 1700. <http://doi.org/10.1039/C1RA00944C>
- X. Ma, A. Zhou, C. Song, *Catal. Today* 123 (2007) 276. <http://dx.doi.org/10.1016/j.cattod.2007.02.036>
- D. Zhao, J. Wang, E. Zhou, *Green Chem.* 9 (2007) 1219. <http://doi.org/10.1039/B706574D>
- H. Lu, J. Gao, Z. Jiang, Y. Yang, B. Song, C. Li, *Chem. Commun.* (2007) 150. <http://doi.org/10.1039/B610504A>
- F. Lin, Y. Zhang, L. Wang, Y. Zhang, D. Wang, M. Yang, J. Yang, B. Zhang, Z. Jiang, C. Li, *Appl. Catal., B* 127 (2012) 363. <http://dx.doi.org/10.1016/j.apcatb.2012.08.024>
- J.M. Campos-Martin, M.C. Capel-Sanchez, P. Perez-Presas, J.L.G. Fierro, *J. Chem. Technol. Biotechnol.* 85 (2010) 879. <http://doi.org/10.1002/jctb.2371>
- D. Huang, Y.J. Wang, Y.C. Cui, G.S. Luo, *Micropor. Mesopor. Mater.* 116 (2008) 378. <http://dx.doi.org/10.1016/j.micromeso.2008.04.031>
- L. Kong, G. Li, X. Wang, B. Wu, *Energy Fuels* 20 (2006) 896. <http://doi.org/10.1021/ef050252r>
- V. Subramanian, E.E. Wolf, P.V. Kamat, *J. Am. Chem. Soc.* 126 (2004) 4943. <http://doi.org/10.1021/ja0315199>
- Y. Tian, T. Tatsuma, *J. Am. Chem. Soc.* 127 (2005) 7632. <http://doi.org/10.1021/ja042192u>
- Y. Ohko, T. Tatsuma, T. Fujii, K. Naoi, C. Niwa, Y. Kubota, A. Fujishima, *Nat. Mater.* 2 (2003) 29.
- U.G. Akpan, B.H. Hameed, *J. Hazard. Mater.* 170 (2009) 520. <http://dx.doi.org/10.1016/j.jhazmat.2009.05.039>
- M. Anpo, M. Takeuchi, *J. Catal.* 216 (2003) 505. [http://dx.doi.org/10.1016/S0021-9517\(02\)00104-5](http://dx.doi.org/10.1016/S0021-9517(02)00104-5)
- E.S. Aazam, *Ceram. Int.* 40 (2014) 6705. <http://dx.doi.org/10.1016/j.ceramint.2013.11.132>
- C. Wang, W. Zhu, Y. Xu, H. Xu, M. Zhang, Y. Chao, S. Yin, H. Li, J. Wang, *Ceram. Int.* 40 (2014) 11627. <http://dx.doi.org/10.1016/j.ceramint.2014.03.156>
- T.H.T. Vu, T.T.T. Nguyen, P.H.T. Nguyen, M.H. Do, H.T. Au, T.B. Nguyen, D.L. Nguyen, J.S. Park, *Mater. Res. Bull.* 47 (2012) 308. <http://dx.doi.org/10.1016/j.materresbull.2011.11.016>
- S. Jeon, C. Lee, J. Tang, J. Hone, C. Nuckolls, *Nano Res.* 1 (2008) 427. <http://doi.org/10.1007/s12274-008-8044-1>
- H. Du, C. Chen, R. Krishnan, T.D. Krauss, J.M. Harbold, F.W. Wise, M.G. Thomas, J. Silcox, *Nano Lett.* 2 (2002) 1321. <http://doi.org/10.1021/nl025785g>
- W. Xiang, C. Xie, J. Wang, J. Zhong, X. Liang, H. Yang, L. Luo, Z. Chen, *J. Alloys Compd.* 588 (2014) 114. <http://dx.doi.org/10.1016/j.jallcom.2013.10.188>
- U. Dasgupta, S.K. Saha, A.J. Pal, *Sol. Energy Mater. Sol. Cells* 124 (2014) 79. <http://dx.doi.org/10.1016/j.solmat.2014.01.041>
- M. Guijun, L. Zhibin, Y. Hongjian, Z. Xu, L. Can, *Chinese. J. Catal.* 30 (2009) 73.
- E.S. Aazam, *J. Ind. Eng. Chem.* 20 (2014) 4008. <http://dx.doi.org/10.1016/j.jiec.2013.12.104>
- X.N. Pham, V.T. Vu, H.V.T. Nguyen, T.T.B. Nguyen, H.V. Doan, *Nanoscale Adv.*, 2022,4, 3600-3608. <https://doi.org/10.1039/D2NA00371F>
- H.V.T. Nguyen, M.B. Nguyen, H.V. Doan, X.N. Pham, *Mater. Res. Express* 10 (2023) 085506. <https://doi.org/10.1088/2053-1591/acf18f>
- N.T.M. Thuy, T.T.K. Chi, U.T.D. Thuy, N.Q. Liem, *Opt. Mater.* 37 (2014) 823. <http://dx.doi.org/10.1016/j.optmat.2014.09.016>
- S.M. Hosseinpour-Mashkani, M. Salavati-Niasari, F. Mohandes, *J. Ind. Eng. Chem.* 20 (2014) 3800. <http://dx.doi.org/10.1016/j.jiec.2013.12.082>
- X.N. Pham, B.M. Nguyen, H.T. Tran, H.V. Doan, *Adv. Powder Technol.* 29 (2018) 1827–1837. <https://doi.org/10.1016/j.apt.2018.04.019>
- X.N. Pham, M.B. Nguyen, H.S. Ngo, H. V. Doan, *J. Ind. Eng. Chem.* 90 (2020) 358–370. <https://doi.org/10.1016/j.jiec.2020.07.037>
- S. Ahmed, M.G. Rasul, W.N. Martens, R. Brown, M.A. Hashib, *Desalination* 261 (2010) 3–18. <https://doi.org/10.1016/j.desal.2010.04.062>